

Numerical simulation of a pyramid steel sheet formed by single point incremental forming using solid-shell finite elements

SheMet'13

Laurent Duchêne¹, **Carlos Felipe Guzmán**¹, Amar Kumar Behera²,
Joost Duflou² and Anne Marie Habraken¹

¹Department ArGENCo, Université de Liège, Belgium.

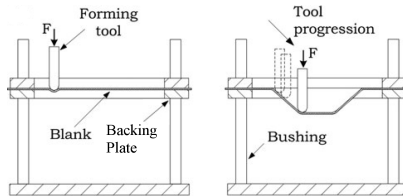
²Department of Mechanical Engineering, Katholieke Universiteit Leuven, Belgium.

March 2013

The logo of KU Leuven, featuring the text 'KU LEUVEN' in white capital letters on a blue rectangular background.

Single point incremental forming

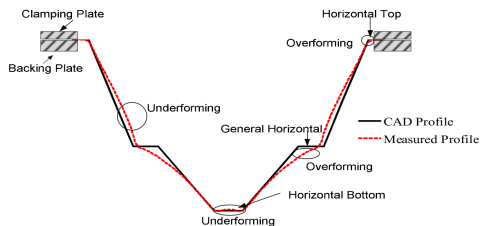
- A sheet metal is deformed by a small tool.
- The tool could be guided by a CNC (milling machine, robot).
- Dieless, with high sheet formability.
- For rapid prototypes, small batch productions, etc.



[Henrard et al., 2010]

Motivations

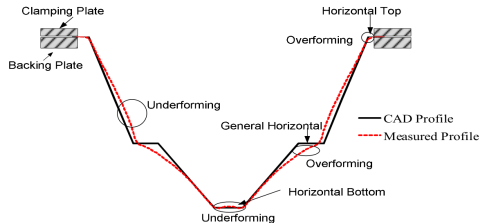
- Geometrical inaccuracy.
- Process mechanics.
- Increased formability.



[Behera et al., 2011]

Motivations

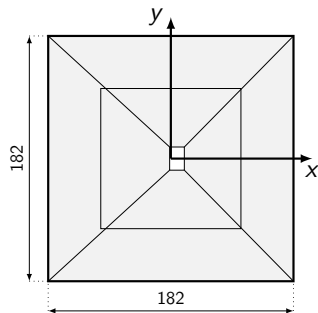
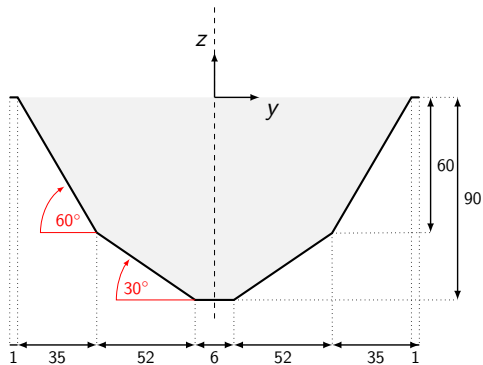
- Geometrical inaccuracy.
- Process mechanics.
- Increased formability.
- Through the thickness gradient are important.
- 2D constitutive laws cannot be used.
- New advances on element formulation in FE codes.



[Behera et al., 2011]

Simulations

- Material: DC01 ferritic steel (1 mm thickness).
- Two slope pyramid:



Constitutive modeling

- Isotropic elasto-plastic constitutive law.
- Voce and Armstrong-Frederick isotropic/kinematic hardening.

$$\sigma_Y = \sigma_{Y0} + K (1 - \exp(-n\epsilon^P))$$

$$\dot{\mathbf{X}} = C_x \left(X_{sat} \dot{\epsilon}^P - \dot{\epsilon}^P \mathbf{X} \right)$$

Constitutive modeling

- Isotropic elasto-plastic constitutive law.
- Voce and Armstrong-Frederick isotropic/kinematic hardening.

$$\sigma_Y = \sigma_{Y0} + K (1 - \exp(-n\epsilon^P))$$

$$\dot{\mathbf{X}} = C_x (X_{sat} \dot{\epsilon}^P - \dot{\epsilon}^P \mathbf{X})$$

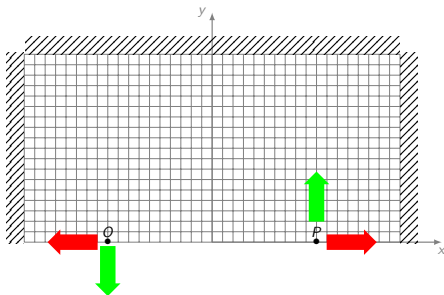
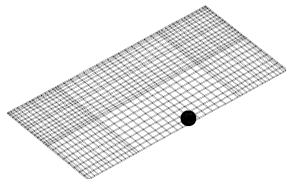
- Material parameters:

$$\begin{array}{llll} \sigma_{Y0} & = & 158 \text{ MPa} & C_x & = & 257 \\ K & = & 255 \text{ MPa} & X_{sat} & = & 4 \text{ MPa} \\ n & = & 13 & & & \end{array}$$

- Identification through *classical* (tensile, monotonic/Bauschinger shear) tests.

Mesh and boundary conditions

- FE code: LAGAMINE.
- Displacement-controlled implicit simulation.
- One layer with 2248 (coarse) and 4282 (fine) elements.
- Symmetry and rotational boundary conditions:

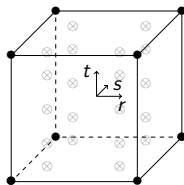


Solid-shell element

SSH3D

- Enhanced assumed strain (EAS).
- Assumed natural strain (ANS).
- In-plane full integration and 5 IP through-the-thickness.

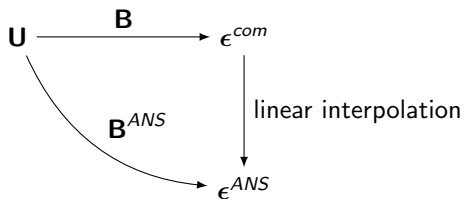
Shell element



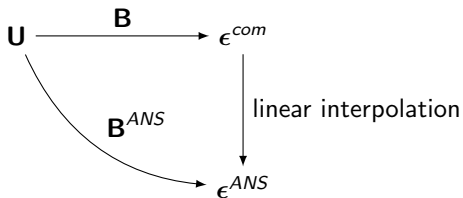
Solid-shell

Brick element

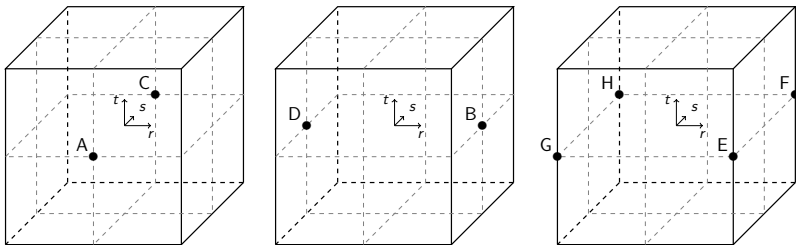
Assumed natural strain



Assumed natural strain



Sampling points (transverse shear and transverse normal strains):



Enhanced assumed strain

Enhanced strain field

$$\boldsymbol{\epsilon} = \boldsymbol{\epsilon}^{com} + \boldsymbol{\epsilon}^{EAS}$$

$$\boldsymbol{\epsilon}^{com} = \Delta^s \mathbf{u} = \mathbf{B}(r, s, t) \mathbf{U}$$

$$\boldsymbol{\epsilon}^{EAS} = \mathbf{G}(r, s, t) \boldsymbol{\alpha} = \frac{|J_0|}{|J(r, s, t)|} \mathbf{F}_0^{-T} \mathbf{M}(r, s, t) \boldsymbol{\alpha}$$

Enhanced assumed strain

Enhanced strain field

$$\epsilon = \epsilon^{com} + \epsilon^{EAS}$$

$$\epsilon^{com} = \Delta^s \mathbf{u} = \mathbf{B}(r, s, t) \mathbf{U}$$

$$\epsilon^{EAS} = \mathbf{G}(r, s, t) \boldsymbol{\alpha} = \frac{|J_0|}{|J(r, s, t)|} \mathbf{F}_0^{-T} \mathbf{M}(r, s, t) \boldsymbol{\alpha}$$

$$[\mathbf{M}] = \begin{bmatrix} r & 0 \\ 0 & s & 0 & 0 & 0 & 0 & 0 & 0 & 0 & 0 & 0 & 0 & 0 & 0 & 0 & 0 & 0 & 0 & 0 & 0 & 0 \\ 0 & 0 & t & 0 & 0 & 0 & 0 & 0 & 0 & 0 & 0 & 0 & 0 & 0 & 0 & 0 & 0 & 0 & 0 & 0 & 0 \\ 0 & 0 & 0 & r & s & 0 & 0 & 0 & 0 & rt & st & 0 & 0 & 0 & 0 & 0 & 0 & 0 & 0 & 0 & 0 \\ 0 & 0 & 0 & 0 & 0 & r & t & 0 & 0 & 0 & 0 & 0 & 0 & 0 & 0 & 0 & 0 & 0 & 0 & 0 & 0 \\ 0 & 0 & 0 & 0 & 0 & 0 & 0 & s & t & 0 & 0 & 0 & 0 & 0 & 0 & 0 & 0 & 0 & 0 & 0 & 0 \end{bmatrix}$$

11 EAS modes

Enhanced assumed strain

Enhanced strain field

$$\epsilon = \epsilon^{com} + \epsilon^{EAS}$$

$$\epsilon^{com} = \Delta^s \mathbf{u} = \mathbf{B}(r, s, t) \mathbf{U}$$

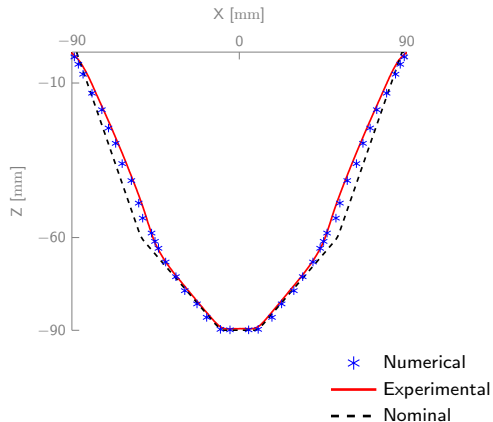
$$\epsilon^{EAS} = \mathbf{G}(r, s, t) \alpha = \frac{|J_0|}{|J(r, s, t)|} \mathbf{F}_0^{-T} \mathbf{M}(r, s, t) \alpha$$

$$[\mathbf{M}] = \begin{bmatrix} r & 0 & 0 & 0 & 0 & 0 & 0 & 0 & 0 & 0 & 0 & 0 & 0 & 0 & 0 & rs & rt & 0 & 0 & 0 & 0 & 0 & 0 & 0 & 0 & rst & 0 & 0 & 0 & 0 & 0 & 0 \\ 0 & s & 0 & rst & 0 & 0 & 0 & 0 \\ 0 & 0 & t & 0 \\ 0 & 0 & 0 & r & s & 0 & 0 & 0 & 0 & rt & st & 0 & 0 & 0 & 0 & 0 & 0 & 0 & 0 & 0 & 0 & 0 & 0 & rs & 0 & 0 & 0 & 0 & 0 & 0 & 0 & 0 & 0 \\ 0 & 0 & 0 & 0 & 0 & r & t & 0 & 0 & 0 & 0 & 0 & rs & st & 0 & 0 & 0 & 0 & 0 & 0 & 0 & 0 & 0 & 0 & 0 & 0 & 0 & 0 & 0 & 0 & 0 & 0 & 0 \\ 0 & 0 & 0 & 0 & 0 & 0 & 0 & s & t & 0 & 0 & 0 & 0 & 0 & 0 & rs & rt & 0 & 0 & 0 & 0 & 0 & 0 & 0 & 0 & 0 & 0 & 0 & 0 & 0 & 0 & 0 & st \end{bmatrix}$$

24 EAS modes

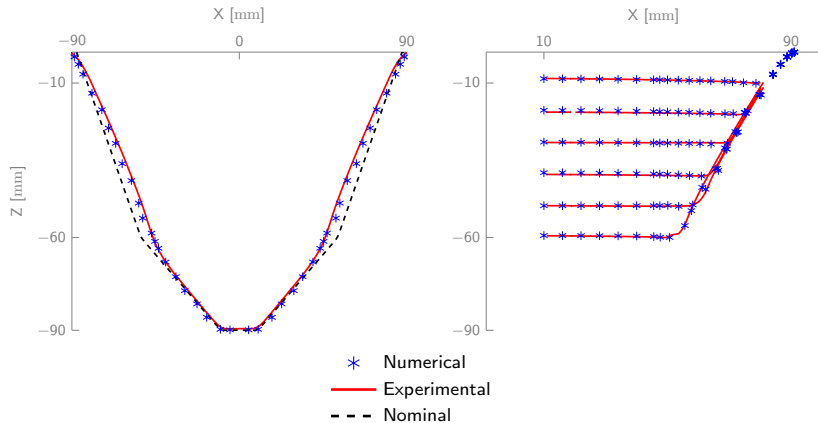
Shape results

Numerical/experimental (DIC) comparison $Y = 0$



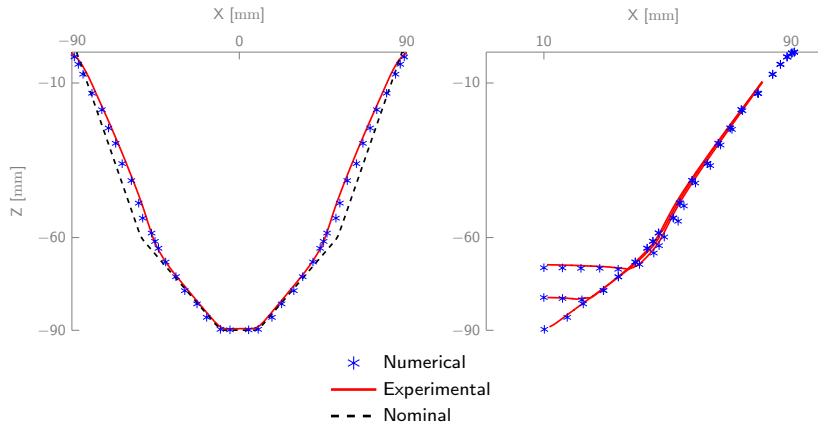
Shape results

Numerical/experimental (DIC) comparison $Y = 0$



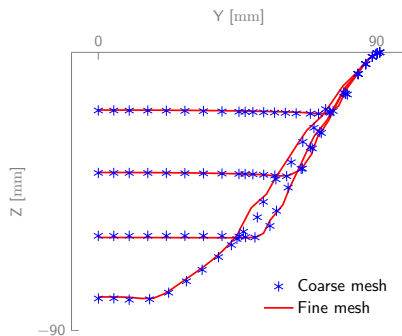
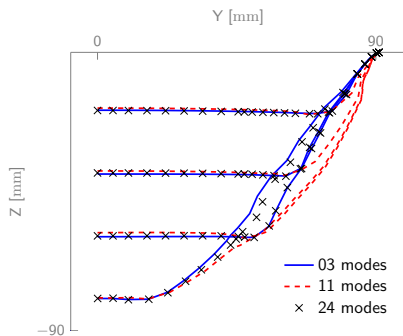
Shape results

Numerical/experimental (DIC) comparison $Y = 0$



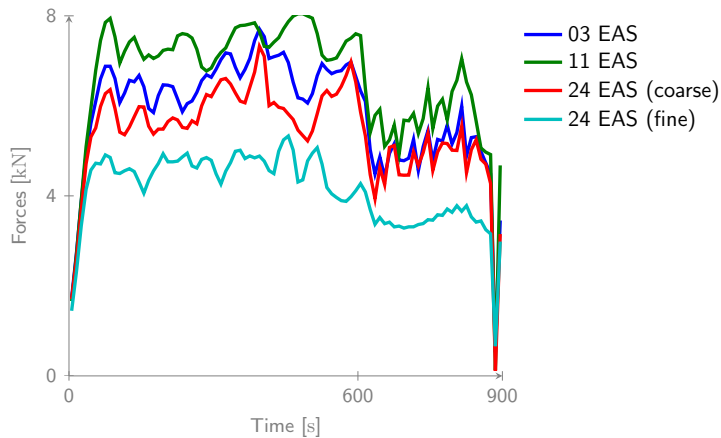
EAS and mesh influence

- Strong EAS mode influence.
- Small mesh influence.



Force evolution

- Both EAS modes and mesh influence.



Conclusions

- EAS modes influence the accuracy of the results.
- The elements are subjected to deformation modes reproduced only using the EAS technique.
- ANS version has no effect on both the shape and the force.
- Material identification procedure important.

Conclusions

- EAS modes influence the accuracy of the results.
- The elements are subjected to deformation modes reproduced only using the EAS technique.
- ANS version has no effect on both the shape and the force.
- Material identification procedure important.

Future work

- Identify the most important EAS modes.
- Improve identification procedure to consider out-of-plane stresses.

Acknowledgments

- Interuniversity Attraction Poles (IAP) Program P7/21 (BelgianScience Policy)



- The Belgian Fund for Scientific Research F.R.S.-FNRS.



References

- Behera, A. K., Vanhove, H., Lauwers, B., Duflou, J., Mar. 2011. Accuracy Improvement in Single Point Incremental Forming through Systematic Study of Feature Interactions. *Key Engineering Materials* 473, 881–888.
- Henrard, C., Bouffioux, C., Eyckens, P., Sol, H., Duflou, J., van Houtte, P., Van Bael, A., Duchêne, L., Habraken, A. M., Dec. 2010. Forming forces in single point incremental forming: prediction by finite element simulations, validation and sensitivity. *Computational Mechanics* 47 (5), 573–590.